CHEMISTRY OF MATERIALS
Article

Chem. Mater. **2010,** *22,* 1585–1594 1585
DOI:10.1021/cm9030182

Solid-State ^{19}F MAS NMR Investigation of Fluoride Ion Mobility in Lead Fluorides: Correlation with Anionic Conductivity

Charlotte Martineau,*[,†,‡,⊥] Franck Fayon,[§] Christophe Legein,[†] Jean-Yves Buzaré,[‡] and Gwenaël Corbel[†]

[†] *Laboratoire des Oxydes et Fluorures (LdOF), CNRS UMR 6010, Institut de Recherche en Ingénierie Moléculaire et Matériaux Fonctionnels (IRIM2F), CNRS FR 2575, Université du Maine, Avenue Olivier Messiaen, 72085 Le Mans Cedex 9, France,* [‡] *Laboratoire de Physique de l'Etat Condensé (LPEC), CNRS UMR 6087, Institut de Recherche en Ingénierie Moléculaire et Matériaux Fonctionnels (IRIM2F), CNRS FR 2575, Université du Maine, Avenue Olivier Messiaen, 72085 Le Mans Cedex 9, France, and* [§] *Conditions Extrêmes et Matériaux: Haute Température et Irradiation (CEMHTI), CNRS UPR 3079, 1D Avenue de la Recherche Scientifique, 45071 Orléans Cedex 2, France and Université d'Orléans, Faculté des Sciences, Avenue du Parc Floral, 45067 Orléans Cedex 2, France.* [⊥] *Current Address: Tectospin, Institut Lavoisier de Versailles (ILV), CNRS UMR 8180, 45 Avenue des États-Unis, 78035 Versailles Cedex, France*

Received September 29, 2009. Revised Manuscript Received December 11, 2009

A study of the fluoride ion mobility in $Pb_5Ga_3F_{19}$ and β-Pb_2ZnF_6, combining data from high-resolution magic-angle-spinning variable-temperature one-dimensional solid-state ^{19}F NMR, two-dimensional exchange NMR experiments, temperature-controlled X-ray diffraction and complex impedance spectroscopy measurements, is presented. In $Pb_5Ga_3F_{19}$, a mutual chemical exchange occurs, above 30 °C, between all the fluorine sites within the isolated $Ga1F_6^{3-}$ octahedra. At higher temperature, a chemical exchange between these ions and some of the free fluoride ions is observed. At least up to 186 °C, fluoride sites belonging to the $Ga2F_6^{3-}$ octahedra chains are not involved in the dynamic process, which results in the absence of anionic conductivity. In β-Pb_2ZnF_6, the fluoride anionic mobility depends on the sample. For $T > 70$ °C, a tridimensional diffusive process takes place in this Aurivillius-type phase due to chemical exchange between the overall fluoride sites, which is confirmed by the occurrence of macroscopic fluoride ionic conductivity.

1. Introduction

Fluoride ion conductors are, to date, the best anionic conductors, due to the small size of the fluoride ion and its single charge,[1] and can therefore be used as solid electrolytes. Variable temperature (VT) ^{19}F nuclear magnetic resonance (NMR) is a relevant technique to study fluoride ion dynamics since the corresponding one-dimensional (1D) NMR spectra are very sensitive to F^- ion motions in the μs−ms scale range.[2] Actually, chemical exchange processes occurring between sites with different chemical shifts modify the NMR line shapes, when the rate of the exchange process enters the so-called intermediate regime of motion. In the case of compounds with multiple sites, magic angle spinning (MAS) is usually required to resolve the resonances of the individual crystallographic sites. Further insights can be obtained with the two-dimensional (2D) exchange spectroscopy (EXSY) NMR experiment.[3] Such MAS NMR studies represent a valuable complement to conductivity measurements and yielded information on the fluoride sites responsible for motion in, for example, α-PbF_2,[4,5] LaF_3,[6] $Ca_{1-x}Y_xF_{2+x}$ ($x = 0.03-0.32$)[7] and $BaSnF_4$.[8]

The structures of $Pb_5Ga_3F_{19}$ and β-Pb_2ZnF_6 were recently resolved[9,10] by combining neutron or X-ray diffraction with multinuclear (^{19}F, ^{207}Pb, ^{71}Ga/^{67}Zn) and multidimensional NMR experiments. During these investigations, we noticed an evolution of the ^{19}F MAS NMR spectra of $Pb_5Ga_3F_{19}$ and β-Pb_2ZnF_6 with the temperature. The present paper is thus devoted to the characterization by solid-state ^{19}F MAS VT and 2D exchange NMR of the fluoride ion mobility in $Pb_5Ga_3F_{19}$ and β-Pb_2ZnF_6. The thermal stability of these compounds was also investigated by temperature-controlled X-ray powder diffraction (XRPD) and complex impedance spectroscopy experiments were carried out up to 320 °C, showing fluorine ionic conduction in β-Pb_2ZnF_6.

*Author to whom correspondence should be addressed. Fax: +33139254476; E-mail: charlotte.martineau@chimie.uvsq.fr.

(1) Hull, S. *Rep. Prog. Phys.* **2004**, *66*, 1233–1314.
(2) Levitt, M. H. *Spin Dynamics: basics of Nuclear Magnetic Resonance*; John Wiley & Sons, LTD: New York, 2000.
(3) Jeener, J.; Meier, B. H.; Bachmann, P.; Ernst, R. R. *J. Chem. Phys.* **1979**, *71*, 4546–4553.
(4) Wang, F.; Grey, C. P. *J. Am. Chem. Soc.* **1995**, *117*, 6637–6638.
(5) Wang, F.; Grey, C. P. *J. Am. Chem. Soc.* **1998**, *120*, 970–980.
(6) Wang, F.; Grey, C. P. *Chem. Mater.* **1997**, *9*, 1068–1070.
(7) Wang, F.; Grey, C. P. *Chem. Mater.* **1998**, *10*, 3081–3091.
(8) Chaudhuri, S.; Wang, F.; Grey, C. P. *J. Am. Chem. Soc.* **2002**, *124*, 11746–11757.
(9) Martineau, C.; Fayon, F.; Legein, C.; Buzaré, J.-Y.; Goutenoire, F.; Suard, E. *Inorg. Chem.* **2008**, *47*, 10895–10905.
(10) Martineau, C.; Fayon, F.; Legein, C.; Buzaré, J.-Y.; Body, M.; Massiot, D.; Goutenoire, F. *Dalton Trans.* **2008**, 6150–6158.

Published on Web 01/07/2010

Finally, on the basis of structural similarities and differences between β-Pb_2ZnF_6 and the low temperature (LT) form of Bi_2WO_6, which is also an anionic conductor with an Aurivillius-type structure, a conduction mechanism is proposed for β-Pb_2ZnF_6.

2. Materials and Methods

2.1. Synthesis. $Pb_5Ga_3F_{19}$ and α-Pb_2ZnF_6 were synthesized as previously reported.[9,10] The starting materials being moisture sensitive, all operations of weighing and grinding were done in a dry glovebox, under nitrogen atmosphere. To ensure that no water remains, the compounds were heated one night at 150 °C under vacuum prior to synthesis realized in sealed platinum tubes. In the PbF_2-ZnF_2 phase equilibrium diagram, the unique binary compound Pb_2ZnF_6 exhibits a reversible $\alpha \rightarrow \beta$ phase transition around 60 °C.[10] Two samples of α-Pb_2ZnF_6 (reported in the following as Pb_2ZnF_6–a and Pb_2ZnF_6–b) were prepared under similar conditions of time and temperature,[10] but using two distinct starting α-PbF_2 (CERAC 135757-B-1B for Pb_2ZnF_6–a and ALFA 213-99-8 for Pb_2ZnF_6–b). The XRPD diagrams recorded for the two starting α-PbF_2 samples and for the two synthesized β-Pb_2ZnF_6 samples were identical. Two samples of $Pb_5Ga_3F_{19}$ were also prepared using the two α-PbF_2 as starting materials. The ^{19}F NMR spectra of the two $Pb_5Ga_3F_{19}$ samples exhibit the same behavior as a function of the temperature and, therefore, only results obtained for the sample synthesized with the CERAC α-PbF_2 batch are presented in this work.

All the experiments detailed in the following that involve β-Pb_2ZnF_6 were carried out starting from α-Pb_2ZnF_6 and heating up the sample to the temperature of the phase transition (or above when necessary).

2.2. NMR Experiments. The ^{207}Pb-decoupled ^{19}F MAS Hahn-echo spectra of $Pb_5Ga_3F_{19}$ and ^{19}F MAS Hahn-echo spectra of β-Pb_2ZnF_6–a were collected on an Avance 400 Bruker spectrometer (B_0 = 9.4 T) operating at ^{19}F Larmor frequency of 376.54 MHz using a ^{19}F optimized CP-MAS probe with a 2.5 mm rotor (spinning frequency up to 35 kHz). We used 2.6 μs 90° pulses, an interpulse delay synchronized with the rotor frequency and recycle delays of 1 s. The ^{207}Pb-decoupled ^{19}F MAS Hahn-echo spectra of β-Pb_2ZnF_6–b and the ^{19}F EXSY spectra of $Pb_5Ga_3F_{19}$ and β-Pb_2ZnF_6–b were recorded on an Avance 300 Bruker spectrometer (B_0 = 7 T, ^{19}F Larmor frequency of 282.2 MHz) equipped with a ^{19}F optimized CP-MAS probe and a 2.5 mm rotor. We employed 2.8 μs 90° pulses. The EXSY spectra were acquired at a temperature of 60 °C and mixing times ranging from 30 μs to 3 ms for $Pb_5Ga_3F_{19}$, and at a temperature of 98 °C and mixing times of 300 μs and 1 ms for β-Pb_2ZnF_6–b. ^{207}Pb continuous wave decoupling was applied in both direct and indirect dimensions. For all experiments, the temperature was monitored using a Bruker cooling unit. ^{207}Pb isotropic chemical shift of $Pb(NO_3)_2$ was used as NMR thermometer.[11,12] The ^{19}F chemical shifts were referenced to $CFCl_3$. All NMR spectra were handled using the DMFIT software.[13]

2.3. X-ray Powder Diffraction. The temperature-controlled X-ray powder diffractograms of $Pb_5Ga_3F_{19}$ and β-Pb_2ZnF_6–b were recorded on a PANalytical θ/θ Bragg-Brentano X'pert MPD PRO diffractometer (Cu $K\alpha_{1+2}$ radiations) equipped with the X'Celerator multi-element detector and an Anton Paar HTK 1200 chamber. Data collection was performed under argon flow at increasing temperature from room temperature (RT) to 430 °C for $Pb_5Ga_3F_{19}$ and from RT to 330 °C for β-Pb_2ZnF_6–b (heating rate 5 °C/min, temperature stabilization for 20 min). At a given temperature, the diffractogram was collected during 79 min in the 20−48° scattering angle range, with a 0.0167° step. A temperature calibration of the chamber was carried out using the structural transitions $\alpha \rightarrow \beta$ and $\beta \rightarrow \gamma$ of $Bi_4V_2O_{11}$ and the brownmillerite to perovskite transition of $Ba_2In_2O_5$.[14] Since the decomposition kinetic of the samples is sensitive to the thermal history (temperature, time, heating/cooling rates), diffraction patterns were collected at the same temperatures as complex impedance spectra were initially recorded, while keeping constant the annealing time and inert atmosphere between both experiments.

2.4. Impedance Spectroscopy Measurements. For conductivity measurements, raw powder samples of $Pb_5Ga_3F_{19}$ and Pb_2ZnF_6–b were shaped as pellets (diameter ~5 mm, thickness ~3 mm) and compacted by means of a uniaxial press (~500 MPa load). The obtained pellets (relative density 85−90% of theoretical density) were characterized without further sintering treatments, owing to the thermal instability of the studied compounds (see below). Thin platinum films were deposited, on each face of the pellets, by radio-frequency sputtering using a Sputter Coater Polaron SC7620 apparatus. The impedance spectra were recorded every 20 °C at increasing temperature from 140 to 320 °C (35 min thermal equilibration) under dry nitrogen flow, using a Schlumberger Solartron 1260 frequency response analyzer connected to a Schlumberger Solartron 1296 dielectric interface over the frequency range 10 MHz to 0.05 Hz (ac signal amplitude of 50 mV, 40 points/decade). The electronic conductivity was measured by the Wagner polarization method on a Schlumberger Solartron 1287/1260 electrochemical response analyzer, in which platinum films were used as ion blocking electrodes, under dry nitrogen flow. Data were analyzed using the Z-view 2.8 d software.[15]

3. Results and Discussion

3.1. NMR Experiments. *3.1.1. $Pb_5Ga_3F_{19}$.* Because the crystalline structure of $Pb_5Ga_3F_{19}$ exhibits a strong static disorder on two of the fluorine atomic positions, two models were proposed to describe the structure:[9] model 1 with strong anisotropic displacement parameters (ADP) on these fluorine positions and model 2 replacing these ADPs by statistic distributions. For the following discussion, we arbitrarily choose the model 1 (ICSD[16] file no. 20110). According to this model, the structure of $Pb_5Ga_3F_{19}$ (Figure 1a) involves two inequivalent octahedral gallium sites, one 10-fold (Pb2) and one 11-fold (Pb1) coordinated lead ions, and seven inequivalent fluorine sites. The structure is built up from a network of both opposite corner-sharing $Ga2F_6^{3-}$ octahedra forming infinite chains along the *c*-axis and isolated $Ga1F_6^{3-}$ octahedra (Figure 1b). Three types of fluoride ions have

(11) Van Gorkom, L. C. M.; Hook, J. M.; Logan, M. B.; Hanna, J. V.; Wasylishen, R. E. *Magn. Reson. Chem.* **1995**, *33*, 791–795.
(12) Bielecki, A.; Burum, D. P. *J. Magn. Reson. Ser. A* **1995**, *116*, 215–220.
(13) Massiot, D.; Fayon, F.; Capron, M.; King, I.; Le Calvé, S.; Alonso, B.; Durand, J. O.; Bujoli, B.; Gan, Z.; Hoatson, G. *Magn. Reson. Chem.* **2002**, *40*, 70–76.
(14) Corbel, G.; Mestiri, S.; Lacorre, P. *Solid State Sci.* **2005**, *7*, 1216–1224.
(15) *Z−view, version 2.8d*; Johnson, D. Scribner Associates Inc.: Southern Pines, NC.
(16) *Inorganic Crystal Structure Database* (*ICSD*), *version 1.4.6*; FIZ Karlsruhe and NIST: Germany and Maryland, 2009.

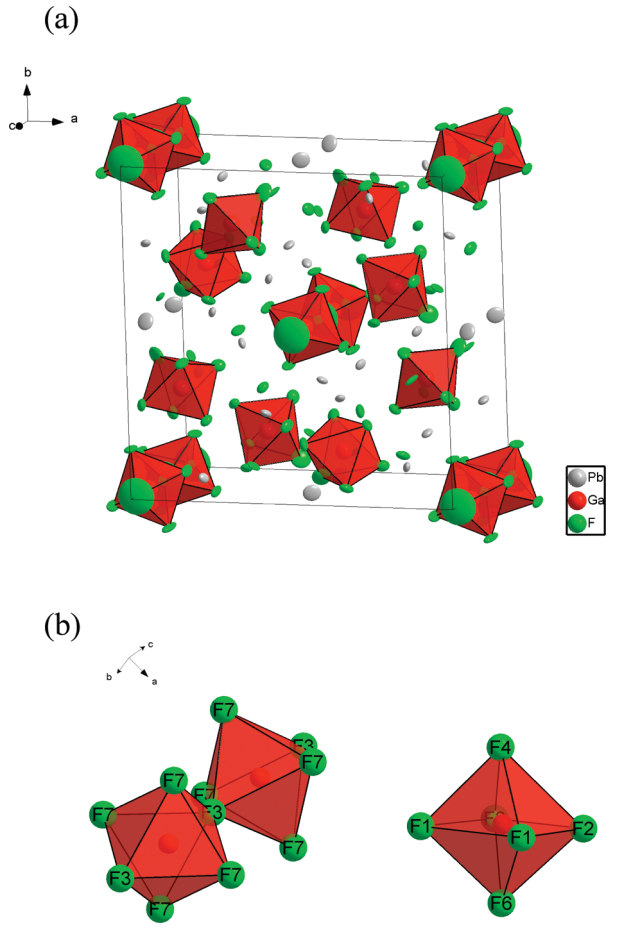

Figure 1. (a) Perspective view of model 1 of the structure of $Pb_5Ga_3F_{19}$. Thermal ellipsoids (50% probability) are represented. (b) Representation of an isolated $Ga1F_6^{3-}$ octahedron (right) and two corner-linked $Ga2F_6^{3-}$ octahedra (left) in $Pb_5Ga_3F_{19}$. Fluorine atoms are labeled.

been distinguished: the bridging fluoride ion F3 that links two $Ga2F_6^{3-}$ octahedra, the non-bridging fluoride ions, F1, F2, F4, F6 that belong to the $Ga1F_6^{3-}$ octahedra and F7 that belong to the $Ga2F_6^{3-}$ octahedra and the "free" fluoride ion F5 that does not belong to any GaF_6^{3-} octahedron. The $Ga2F_6^{3-}$ octahedra are tilted within the chains, as reflected by the strong static disorder on the position of F3 and F7.[9]

In Figure 2 are displayed the ^{207}Pb decoupled ^{19}F MAS spectra of $Pb_5Ga_3F_{19}$, recorded at temperature ranging from 28 to 186 °C. The assignment of the RT (28 °C) spectrum was recently proposed[9] and is reported in Figure 2. As temperature increases, the peaks corresponding to the fluoride ions F1, F2, F4, and F6 broaden (for example the line width of the F6 resonance increases from 1.8 kHz at 28 °C to 3.0 kHz at 57 °C), indicating that these fluoride ions are experiencing a motion at a rate close to the difference of chemical shift, in frequency, between these sites (i.e., the intermediate regime of motion). Then, as temperature, thus the rate of motion, increases further, the peaks coalesce in a peak labeled B. This peak is centered at −100 ppm, that is, the weighed mean of the isotropic chemical shifts at RT of the peaks which coalesce (Table 1). This indicates that F1, F2, F4, and F6 ions, which are located at the six corners of the

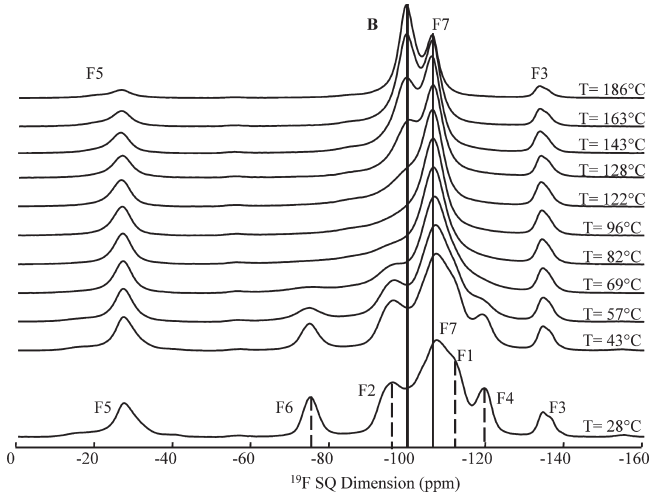

Figure 2. VT (28−186 °C) ^{19}F MAS (30 kHz) Hahn-echo spectra of $Pb_5Ga_3F_{19}$ recorded at 9.4 T with ^{207}Pb decoupling. ^{19}F NMR lines are assigned.[9] Dash lines indicate the position of the non-bridging fluoride ions F4, F1, F2, and F6 at 28 °C. The narrow line indicates position of the non-bridging F7 fluoride ions and the thick one the position of the line labeled B.

Table 1. Line Assignment, Isotropic Chemical Shift δ_{iso} (ppm) and Relative Multiplicity of the Fluorine Sites in $Pb_5Ga_3F_{19}$[9]

line assignment	F3		F4	F1	F7	F2	F6	F5
δ_{iso} (±1 ppm)	−137	−133	−119	−110	−105	−96	−75	−28
relative multiplicity	0.5		1	2	2	2	1	1

isolated $Ga1F_6^{3-}$ octahedra (Figure 1b), are all involved in a chemical exchange. The correlation time at coalescence (82 °C < T < 96 °C) is a function of the chemical shift difference ($\Delta\nu$ = 16.5 kHz): $\tau_c = \sqrt{2}/\pi\Delta\nu = 2.7 \times 10^{-5}$ s. For higher temperature (until T = 186 °C, the maximum temperature investigated), the width of line B decreases. This motional narrowing indicates that the fast exchange regime is reached. One can notice that the line assigned to the free fluoride ions F5 broadens at temperature above 122 °C, which could correspond to a motion of these fluoride ions. However, this line does not merge with line B, thus this motion likely occurs at a distinct rate. The lines assigned to the fluoride ions F3 and F7 belonging to the $Ga2F_6^{3-}$ octahedra do not evolve significantly with temperature, indicating that they are not involved in the dynamic process, at least, for temperature below 186 °C. The ^{19}F MAS NMR spectra were also collected on cooling (not shown) and, for a given temperature, they were identical to the spectra recorded on heating. The heating−cooling cycle was repeated several times for selected temperatures, each times showing the same change in NMR line shape. This indicates that the process is reversible without hysteresis.

The fluoride ion motion was further investigated using ^{19}F 2D NMR EXSY experiments. The spectra recorded at a temperature of 60 °C and with different mixing times are shown in Figure 3. The ^{19}F chemical shift range being too large to allow rotor-synchronization, spinning sidebands occur in both horizontal and vertical dimensions of the 2D spectra. At short mixing delay (30 μs),

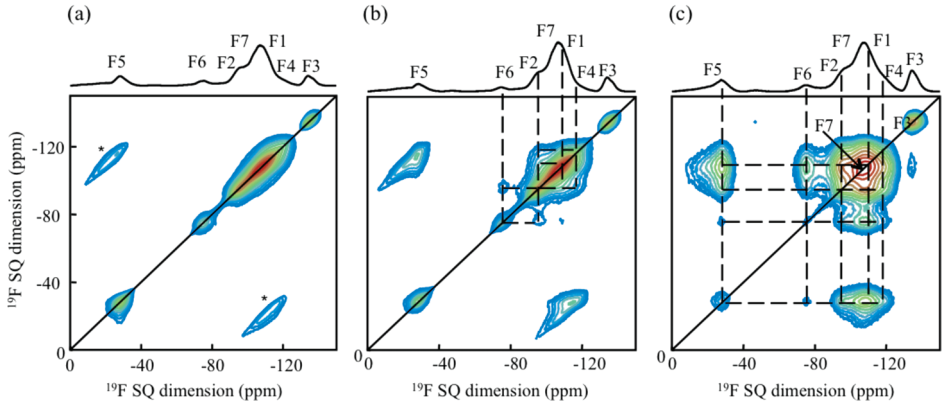

Figure 3. 2D ^{19}F MAS (25 kHz) EXSY spectra of $Pb_5Ga_3F_{19}$ recorded at 7 T, at a temperature of 60 °C and with mixing time of (a) 30 μs, (b) 150 μs and (c) 3 ms. Top spectra, on which ^{19}F NMR lines are labeled, are the full projection on the ^{19}F MAS dimension. The thick solid line indicates the diagonal of the spectra; dash lines show fluorine-fluorine cross-correlations, and stars indicate the position of the spinning sidebands.

the spectrum shows off diagonal peaks, which correspond to the spinning sidebands (Figure 3a). For a longer mixing time of 150 μs (Figure 3b), cross-peaks between the resonances corresponding to the adjacent F^- sites within the $Ga1F_6^{3-}$ octahedron (Figure 1b) are observed. It should be mentioned that cross-correlation peaks between ^{19}F resonances in EXSY experiments can either be due to chemical exchange or ^{19}F spin diffusion (which corresponds to magnetization transfer through homonuclear dipolar couplings depending on the chemical shift difference between the dipolar-coupled nuclei).[17−20] Under fast MAS condition, the spin diffusion process is significantly slowed down when rotational resonance conditions are avoided.[20,21] Therefore the cross-correlation peaks observed for $Pb_5Ga_3F_{19}$ at a MAS frequency of 25 kHz for the short mixing time employed here (150 μs) likely reveal chemical exchange on the time scale of the mixing time (i.e., $\tau_c < 15 \times 10^{-5}$ s). The spectrum recorded with the longest mixing time (Figure 3c) also evidence cross-peaks between opposite F^- (F4 and F6) ions within a $Ga1F_6^{3-}$ octahedron (Figure 1b). This exchange only appears for longer mixing time since it requires two successive jumps between two adjacent F^- sites. Cross-peaks between the F1, F2, F4, and F6 ions and the free fluoride ions F5 are also present, indicating that F5 ions are also partly involved in the chemical exchange process. The ^{19}F 1D MAS NMR spectrum gives no evidence for this exchange at this temperature, very likely because 1D MAS NMR experiments probe shorter correlation times than the EXSY experiments. Finally, the 2D EXSY spectrum shows exclusively diagonal peaks for F7 and F3, confirming that they do not take part in the exchange.

The lack of any other resonances which could be assigned to interstitial fluoride sites, and the observation of a resonance which is intermediate in frequency between the resonances of the non-bridging F1, F2, F4, F6 fluoride ions, suggest that the motion of these ions and the motion of the free F5 fluoride ions do not involve interstitial fluoride ions. Since the $Ga1F_6^{3-}$ octahedra are isolated, the motion observed between the F1, F2, F4, and F6 ions do not concern fluoride ions from different $Ga1F_6^{3-}$ octahedra but comes from a mutual exchange between all these fluoride ions within a $Ga1F_6^{3-}$ octahedron. It can also be explained as a rotation of the whole $Ga1F_6^{3-}$ octahedra, as was observed for AlF_6^{3-} octahedra in Na_3AlF_6.[22] On the other hand, the motion between these F^- ions and some of the free fluorides F5 could originate from anionic vacancies. Since $Pb_5Ga_3F_{19}$ is pure and since the static disorder only concerns non-mobile F3 and F7, the presence of anion vacancies very likely originate from Schottky type point defect. The F^- motions observed here are probably favored by the high polarizability of the Pb^{2+} ions within the immobile sublattice, which can deform to allow the rotation of the whole $Ga1F_6^{3-}$ octahedra and the diffusion of fluoride ions.[1] The short distances between the adjacent F^- ions within the $Ga1F_6^{3-}$ octahedra (Table 2) facilitate the motion observed between these fluoride ions. The partial chemical exchange between F5 and these fluoride ions may be related to longer distances, on average (Table 2). Finally, the absence of chemical exchange between, in the one hand, F5 and F^- ions from the $Ga1F_6^{3-}$ octahedra and, in the other hand, F^- ions from the $Ga2F_6^{3-}$ octahedra, may be due to mostly long F−F distances.

While there is a static structural disorder that concerns the $Ga2F_6^{3-}$ octahedra files[9] in $Pb_5Ga_3F_{19}$, this VT ^{19}F NMR investigation shows a distinct and dynamic phenomenon: the chemical exchange between all fluoride ions of $Ga1F_6^{3-}$ octahedra and a part of the free fluoride ions.

3.1.2. β-Pb_2ZnF_6. The crystal structure of the high temperature phase (β-) of Pb_2ZnF_6 has recently been determined (ICSD[16] file no. 162074) and optimized (ICSD[16] file no. 162073).[10] In the following, all the discussed structural data (interatomic distances and bond angles) were calculated

(17) Suter, D.; Ernst, R. R. *Phys. Rev. B* **1985**, *32*, 5608–5627.
(18) Henrichs, P. M.; Linder, M.; Hewitt, J. M. *J. Chem. Phys.* **1986**, *85*, 7077–7086.
(19) Kubo, A.; McDowell, C. A. *J. Chem. Phys.* **1988**, *89*, 63–70.
(20) Du, L.-S.; Levitt, M. H.; Grey, C. P. *J. Magn. Reson.* **1999**, *140*, 242–249.
(21) Reichert, D.; Bonagamba, T. J.; Schmidt-Rohr, K. *J. Magn. Reson.* **2001**, *151*, 129–135.
(22) Kotecha, M.; Chaudhuri, S.; Grey, C. P.; Frydman, L. *J. Am. Chem. Soc.* **2005**, *127*, 16701–16712.

Table 2. F—F Distances (Å) d_{F-F} (< 3.5 Å) in $Pb_5Ga_3F_{19}$ (Calculated from Model 1)[9]

atom	atom	d_{F-F}	atom	atom	d_{F-F}	atom	atom	d_{F-F}
F1	F2	2.6279	F2	F1	2.9369	F5	F1	3.0721 (×2)
	F6	2.6373		F5	2.9848		F2	3.0901 (×2)
	F4	2.6479		F5	3.0901	F6	F2	2.6011 (×2)
	F4	2.8976		F6	3.2791		F1	2.6373 (×2)
	F2	2.9369	F3	F7	2.5893 (×4)		F5	2.8867 (×2)
	F1	2.9582		F7	2.6432 (×4)		F5	2.977
	F7	2.9914	F4	F1	2.6479 (×2)		F6	3.0657
	F5	3.0721		F5	2.7733		F2	3.2791 (×2)
	F7	3.2169		F2	2.8077 (×2)	F7	F3	2.5893
	F7	3.2498		F1	2.8976 (×2)		F7	2.6037 (×2)
F2	F6	2.6011	F5	F4	2.7733		F3	2.6432
	F2	2.6115		F6	2.8867 (×2)		F2	2.6677
	F1	2.6279		F6	2.977		F1	2.9914
	F7	2.6677		F2	2.9848 (×2)		F1	3.2169
	F4	2.8077		F2	2.9848		F1	3.2498

from the optimized structure of β-Pb_2ZnF_6. It involves one octahedral zinc site, one 11-fold coordinated lead ion (d_{Pb-F} < 3.24 Å) and five inequivalent fluorine sites and is built from alternated layers parallel to the (*a*,*b*) plane (Figure 4): tilted layers $[ZnF_4]^{2-}$ of corner-sharing ZnF_6^{4-} octahedra and layers $(FPb)^+$ of edge-sharing FPb_4^{7+} tetrahedra. Then, the structure has one non-bridging fluoride ion (F1) and two bridging fluoride ions (F2 and F3), located in the $[ZnF_4]^{2-}$ layers, as well as two free fluoride ions (F4 and F5), located in the $(FPb)^+$ layers.

The VT ^{19}F MAS NMR study has been carried out on two samples β-Pb_2ZnF_6–a and β-Pb_2ZnF_6–b. As mentioned in the experimental section, both samples were synthesized under similar temperature and time conditions, but using different α-PbF_2 samples as starting materials.

The striking point is that the evolution of the VT ^{19}F MAS NMR spectra of β-Pb_2ZnF_6 depends on the sample. While the VT ^{19}F MAS NMR spectra of the sample β-Pb_2ZnF_6–a show no significant evolution with increasing temperature (Figure 5), the VT ^{19}F MAS NMR spectra of sample β-Pb_2ZnF_6–b are much more sensitive (Figure 6). At T = 69 °C, the spectrum of β-Pb_2ZnF_6–a shows four ^{19}F resonances, previously assigned[10] to the free (F4 and F5), non-bridging (F1) and bridging (F2 and F3) fluorine sites (Table 3). The ^{19}F MAS spectrum of β-Pb_2ZnF_6–b, recorded at the same temperature (72 °C), exhibits two additional resonances labeled A and B (Figure 6). The position of line A (−113 ppm) is roughly the weighed mean (−116 ppm) of the isotropic chemical shifts of the non-bridging (F1) and bridging (F2 and F3) fluoride ions, while the position of line B (−85 ppm) is the weighed mean of the isotropic chemical shifts of all fluoride ions. Therefore, these extra lines give evidence for chemical exchange processes through anion vacancies (between the F1, F2 and F3 fluoride ions located in the $[ZnF_4]^{2-}$ layers in the one hand and between all the fluoride ions on the other hand) with distinct rates of motion. It should be mentioned that the RT ^{19}F MAS NMR spectra (not shown) of the two α-PbF_2 samples used for the syntheses of β-Pb_2ZnF_6–a and –b are identical and each exhibits two resonances of equal intensities

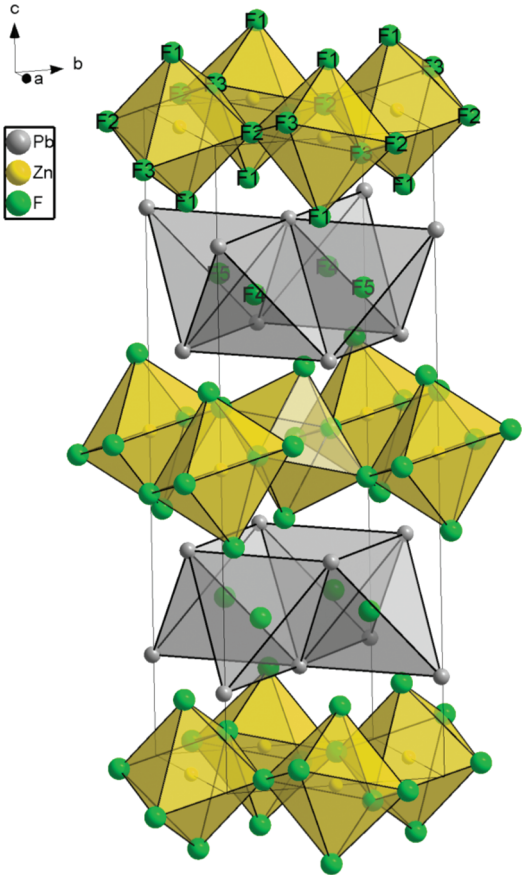

Figure 4. Perspective view of the structure of β-Pb_2ZnF_6. Fluorine atoms are labeled.

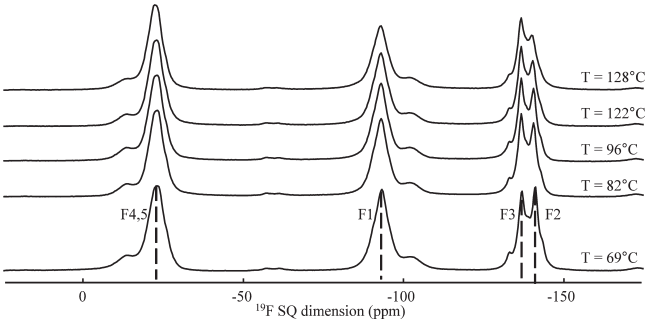

Figure 5. VT (69 to 128 °C) ^{19}F MAS (30 kHz) Hahn-echo spectra of β-Pb_2ZnF_6–a recorded at 9.4 T without ^{207}Pb decoupling. ^{19}F NMR lines are assigned.[10] Non-labeled peaks are spinning sidebands.

corresponding to the two fluorine crystallographic sites of the structure (ICSD[16] file no. 14324).[23] This clearly indicates that the two α-PbF_2 samples are free of impurities such as monovalent cations and/or oxide ions that would generate anionic vacancies and thus fluoride and/or mixed oxide-fluoride ion mobility resulting in extra NMR line on the ^{19}F MAS NMR spectrum as observed in reference 5 (α-PbF_2 containing trace amounts of potassium or doped with KF). A priori, one could also suspects the presence of trace amounts of hydroxide (F^-/OH^- substitution) in the α-PbF_2 samples and consequently in β-Pb_2ZnF_6. However, this isovalent F^-/OH^- substitution do not create vacancy, thus cannot generate extra fluoride ion mobility. Therefore, the presence of

(23) Boldrini, P.; Loopstra, B. O. *Acta Crystallogr.* **1967**, *22*, 744–746.

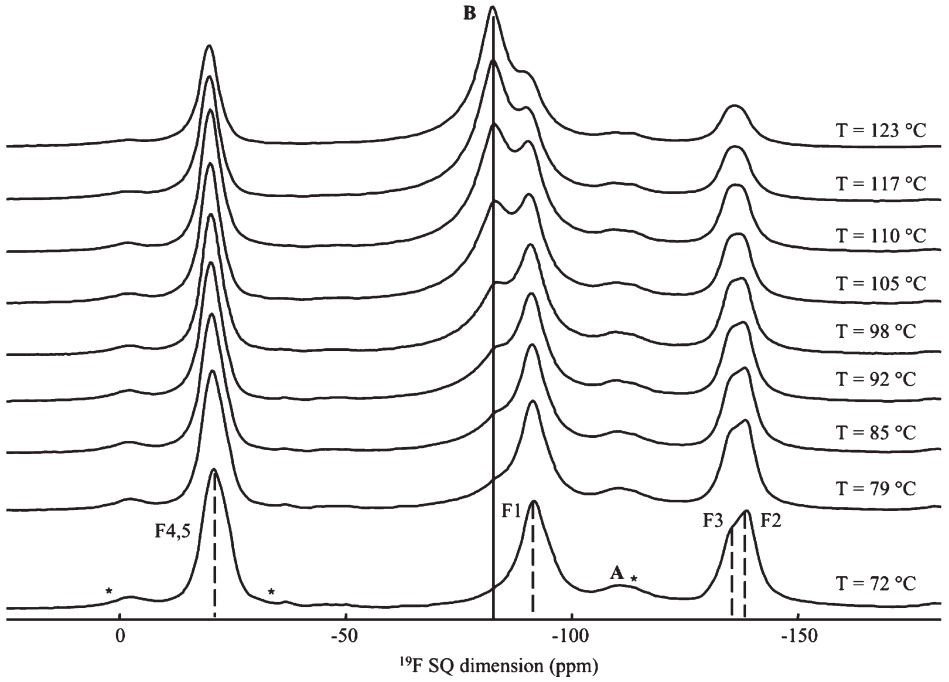

Figure 6. VT (72−123 °C) ^{19}F MAS (25 kHz) Hahn-echo spectra of β-Pb_2ZnF_6–b recorded at 7 T with ^{207}Pb decoupling. ^{19}F NMR lines are assigned.[10] Stars show the position of spinning sidebands. Dash lines indicate the line positions at 72 °C. The thick line indicates position of the line labeled B.

Table 3. Line Assignment, Isotropic Chemical Shift δ_{iso} (ppm), and Relative Multiplicity of the Fluorine Sites in β-Pb_2ZnF_6[10]

line assignment	F2	F3	F1	F4 and F5
δ_{iso} (±1 ppm)	−141	−136	−93	−23
relative multiplicity	1	1	2	2

vacancies in β-Pb_2ZnF_6 very likely originates from Schottky type point defects.

The fluoride ions corresponding to lines A and B on the ^{19}F MAS NMR spectra of β-Pb_2ZnF_6–b are in the intermediate regime of motion, that is, are undergoing rapid jumps between the crystallographic sites at frequencies that are larger than the frequency separation of the resonances: ∼13 kHz between F1 and F2 and ∼33 kHz between (F4, F5) and F2, which correspond to correlation times τ_c smaller than 3.5×10^{-5} s and 1.4×10^{-5} s, respectively. The other F^- ions corresponding to the F1 to (F4, F5) resonances (with linewidths that do not vary with the temperature) are in the slow regime of motion. Here, the simultaneously occurrence of F1 to (F4, F5) and of the A and B resonances in the ^{19}F spectra of β-Pb_2ZnF_6–b resulting from multiple regime of ^{19}F motion can only be explained considering either at least two relatively narrow distributions or a broad distribution of motional correlation times. The fastest moving fluoride ions (corresponding to lines A and B) most likely sit close to a vacancy. The relative intensity of line A is nearly constant over the investigated temperature range and is around 5% of the total fluoride ions (i.e., 7.5% of the non-bridging and bridging fluoride ions). The relative intensity of line B, which represents the fraction of the total fluoride ions that are mobile, increases linearly with temperature (Figure 7). By extrapolation, the totality of the fluoride ions is thus estimated to be in the intermediate

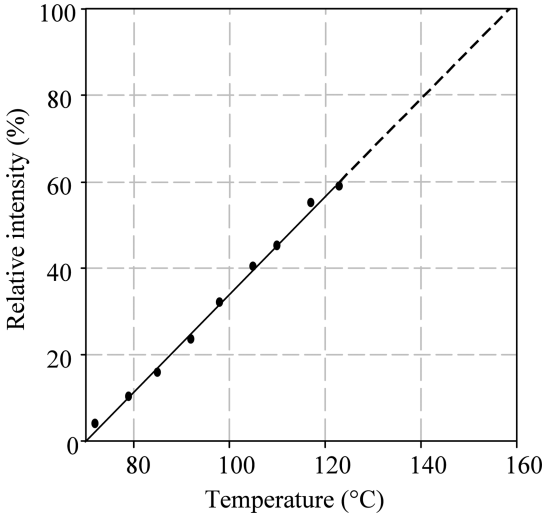

Figure 7. Relative intensity (%) of the line B in β-Pb_2ZnF_6–b plotted vs temperature (°C). The solid line corresponds to the linear regression (relative intensity = 1.127 × T (°C) − 78.65, r^2 = 0.996) and the dashed line to its extrapolation.

regime of motion around 160 °C. The ^{19}F MAS NMR spectra of β-Pb_2ZnF_6–b recorded on cooling show that the motional process is reversible without hysteresis.

To obtain further information about the correlation time in the slow regime of motion, ^{19}F MAS EXSY spectra of β-Pb_2ZnF_6–b were recorded at a temperature of 98 °C. As already mentioned, ^{19}F spin diffusion can be reasonably neglected for the very short mixing time (300 μs to 1 ms) employed here under fast MAS condition (spinning frequency of 25 kHz). In Figure 8a, cross-correlation peaks between the (F4, F5) and F1 as well as between the F2 and F3 resonances are observed for a mixing time of 300 μs indicating that these rigid fluoride

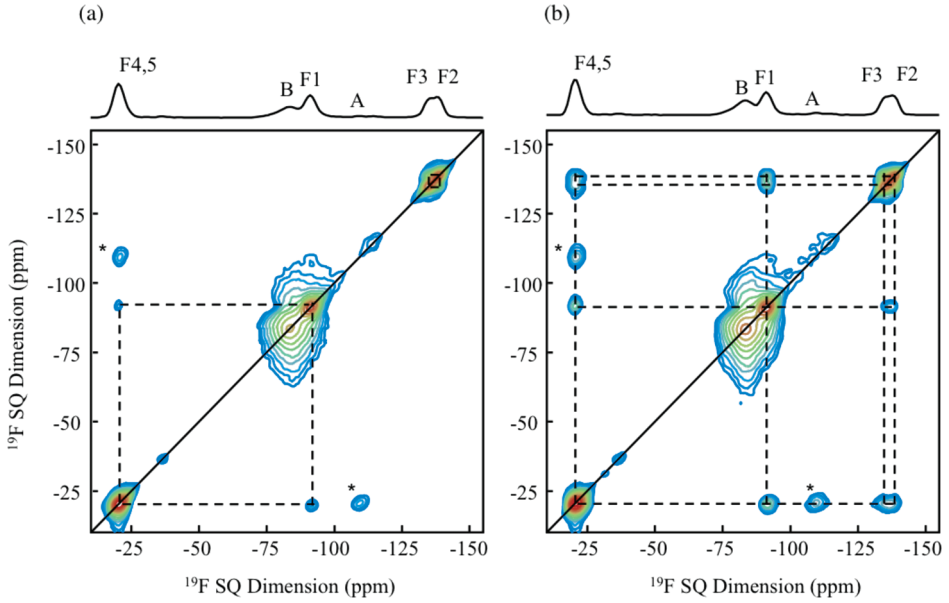

Figure 8. 2D ^{19}F MAS (25 kHz) EXSY spectra of β-Pb_2ZnF_6–b recorded at 7 T at a temperature of 98 °C and a mixing time of (a) 300 μs and (b) 1 ms. Top spectra, on which ^{19}F NMR lines are labeled, are the full projection on the ^{19}F MAS dimension. The thick solid lines indicate the diagonal of the spectra, while the dash lines show fluorine−fluorine cross-correlations. Stars indicate spinning sidebands.

ions are involved in a chemical exchange with a correlation time of about 30×10^{-5} s at 98 °C, i.e. more than 1 order of magnitude larger than that of the intermediate regime of motion. It should be pointed out that the cross-correlation peaks corresponding to the chemical exchange between the free F^- ions (F4 and F5) and the equatorial F2 and F3 ions of the ZnF_6^{4-} octahedra only appear for a longer mixing time of 1 ms (Figure 8b) since it requires successive hops through the position of the axial F1 fluoride ions (Figure 4).

NMR results show two distinct chemical exchange processes through F vacancies: a bidimensional one between F1, F2, and F3 in the ZnF_6^{4-} octahedron layers, and a tridimensional one involving all fluoride ions, both of them having either at least two relatively narrow distribution or a broad distribution of motional correlation times. It is difficult to explain the different behavior between the _a and _b β-Pb_2ZnF_6 samples. However, the occurrence of the F vacancies in the ZnF_6^{4-} octahedron layers in β-Pb_2ZnF_6, shown by the line A on the ^{19}F MAS NMR spectrum of the _b sample, seems to be the factor that gives rise to the ionic mobility.

Regarding the mobility of the fluoride ions observed by NMR, complex impedance spectroscopy experiments have been carried out on $Pb_5Ga_3F_{19}$ and β-Pb_2ZnF_6–b to look for possible anionic conductivity properties.

3.2. Thermal Stability and Anionic Conductivity. *3.2.1. Thermal Instability of the Samples.* The thermodiffractograms of the powder samples β-Pb_2ZnF_6, recorded between 75 and 330 °C (Figure 9) show the partial decomposition of the samples, for temperature above 280 °C, into a phase which diffraction reflections are characteristic of a fluorite type β-PbF_2 structure (PDF[24] file no. 00-006-0251, ICSD[16] file no. 53984).[25] XRPD diagram (not shown) was then recorded at 25 °C following the thermodiffraction experiments. The diagram show the presence of α-Pb_2ZnF_6 and of a similar amount of the β-PbF_2-type structure compound as on the diagrams recorded at 330 °C, indicating that the decomposition is irreversible. XRPD experiments were also run on the top surface and the core of pellets previously studied by complex

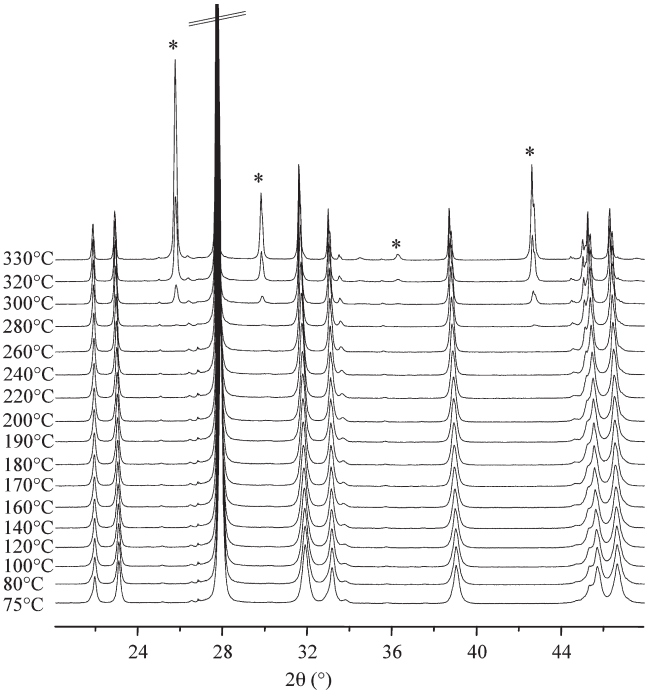

Figure 9. Temperature controlled XRPD diagrams of β-Pb_2ZnF_6–b recorded between 75 and 330 °C. Stars indicate the reflection peaks of a fluorite type β-PbF_2 phase (PDF[24] file no. 00-006-0251, ICSD[16] file no. 53984) resulting from the partial decomposition of the sample.

(24) *PDF−4+2007*; The International Centre for Diffraction Data (ICDD): Newtown Square, PA, 2007.

(25) Ito, Y.; Koto, K. *Solid State Ionics* **1983**, *9*, 527–530.

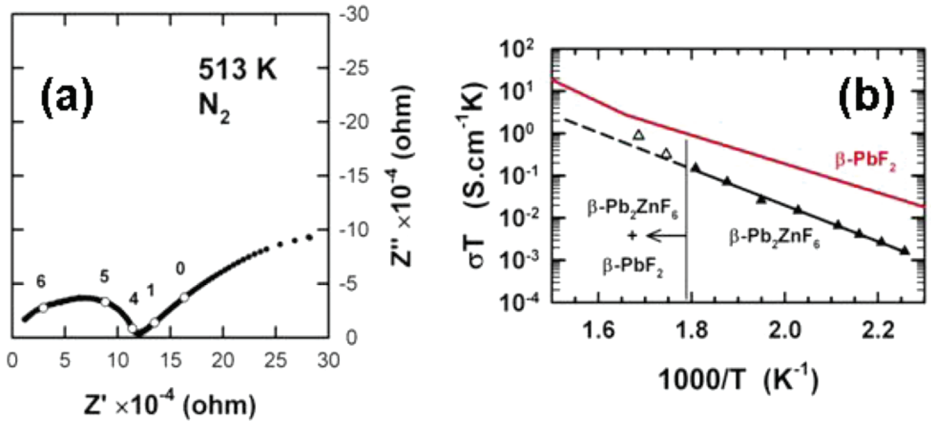

Figure 10. (a) Representative Nyquist plot of complex impedance spectrum collected at 513 K on ceramic of β-Pb_2ZnF_6–b in N_2 (numbers correspond to frequency logarithms). (b) Temperature dependence of the electrical conductivity of β-Pb_2ZnF_6–b fitted with a conventional Arrhenius law in the temperature range 413−553 K (solid black line). Above 553 K (open triangles), the divergence from linearity is ascribed to the occurrence of β-PbF_2 type phase arising from the partial decomposition of β-Pb_2ZnF_6–b, evidenced by temperature-controlled X-ray diffraction. For comparison, the conductivity curve of pure β-PbF_2 reported by Bonne et al.[26] is added on the figure.

impedance spectroscopy. The diagrams (not shown) reveal that the decomposition only occurs on the top, bottom, and lateral surfaces (on about 0.3 mm of thickness) of the pellets.

A similar thermodiffraction study (thermodiffractograms not shown) was also carried out recorded on powder samples and pellets of $Pb_5Ga_3F_{19}$ showing an analogous irreversible decomposition, at temperature slightly different (290 °C), of the compound in a β-PbF_2-type phase.

The partial and irreversible decomposition of the compounds into β-PbF_2 probably originates from the existence of Schottky type point defects (cationic and anionic vacancies $V_{Pb} + 2V_F$) formed by moving the constituent Pb^{2+} and F^- ions to the surface from their bulk sites.

3.2.2. Complex Impedance Spectroscopy. No anionic conductivity is measured for $Pb_5Ga_3F_{19}$ for temperatures below the temperature of decomposition (290 °C), which was expected since the chemical exchange observed on the ^{19}F MAS NMR spectra is occurring mostly between the fluoride ions within the isolated $Ga1F_6^{3-}$ octahedra.

The complex impedance spectrum of β-Pb_2ZnF_6–b recorded at 240 °C is presented in Figure 10a. As shown in this figure, a polarization phenomenon associated with fluoride ion conduction between the sample and the platinum electrodes is clearly detected at the low frequency side of the spectrum. This polarization is only detected above 160 °C in good agreement with the temperature estimated from the ^{19}F MAS NMR spectra at which all fluoride ions are expected to be mobile. At high frequency, the impedance spectrum exhibits two overlapping semicircles, which can be satisfactorily least-squares adjusted with a series combination of one $R//C$ and one $R//$CPE elements of the Z-view 2.8d software[15] (where R and C are pure resistance and capacitance, respectively, and CPE is a constant phase element). On the basis of the values of capacitance, the former arc modeled with a $R//C$ element (~4.5×10^{-12} to 3.5×10^{-11} F) was assigned to the bulk response, whereas the latter arc (~1×10^{-10} to 1.0×10^{-9} F) was associated to the grain boundaries contribution. In the temperature range 170−280 °C, the temperature dependence of the total electric conductivity, σ, is modeled with a conventional Arrhenius law: $\log(\sigma T) = \log(\sigma_0) - Ea/RT$, with $\log \sigma_0 = 6.89\ S \cdot K \cdot cm^{-1}$ and the activation energy $E_a = 0.85$ eV. As highlighted by temperature-controlled X-ray diffraction, a partial decomposition of β-Pb_2ZnF_6–b takes place above 280 °C (Figure 9). The progressive increase of the amount of the β-PbF_2 type phase with increasing temperature is responsible for the smooth rise in conductivity (open triangles in Figure 10b) since this latter phase is a slightly better fluoride ionic conductor[26] than β-Pb_2ZnF_6–b (Figure 10b). In β-Pb_2ZnF_6–b, very low electronic conductivities ($\sigma_e \sim 1.3 \times 10^{-10}\ S \cdot cm^{-1}$ and ~$1.6 \times 10^{-10}\ S \cdot cm^{-1}$ at 170 and 240 °C, respectively) were measured by the Wagner polarization method. The conductivity in β-Pb_2ZnF_6 is therefore considered as almost purely anionic since the value of the ionic transference $t_F = 1 - \sigma_e/\sigma_{total}$ is very close to the unity. However, the ionic conductivity of β-Pb_2ZnF_6 (σ (200 °C) = $1.39 \times 10^{-5}\ S \cdot cm^{-1}$) is 4 orders of magnitude lower than the value reported for the faster fluoride ionic conductor β-$PbSnF_4$ (σ (200 °C) ~ $10^{-1}\ S \cdot cm^{-1}$).[27]

3.3. Conduction Mechanism in β-Pb_2ZnF_6. In an attempt to find structural keys that could explain the anionic conductivity measured in β-Pb_2ZnF_6, a deeper structural analysis has been carried out. The β-form adopts an Aurivillius-type structure, similar to the structure of oxide ion conductors, as for instance the LT-form of Bi_2WO_6 (Figure 11)[28,29] and β- and γ-$Bi_4V_2O_{11}$, which are intrinsic oxygen deficient related compound belonging to the $BiMeVO_x$ family.[30−32]

(26) Bonne, R. W.; Schoonman, J. *J. Electrochem. Soc.* **1977**, *124*, 28–35.
(27) Réau, J.-M.; Lucat, C.; Portier, J.; Hagenmuller, P.; Cot, L.; Vilminot, S. *Mater. Res. Bull.* **1978**, *13*, 877–882.
(28) Knight, K. S. *Mineral. Mag.* **1992**, *56*, 399–409.
(29) Islam, M. S.; Lazure, S.; Vannier, R.-N.; Nowogrocki, G.; Mairesse, G. *J. Mater. Chem.* **1998**, *8*, 655–660.
(30) Abraham, F.; Debreuille-Gresse, M. F.; Mairesse, G.; Nowogrocki, G. *Solid State Ionics* **1988**, *28−30*, 529–532.
(31) Abraham, F.; Boivin, J.-C.; Mairesse, G.; Nowogrocki, G. *Solid State Ionics* **1990**, *40−41*, 934–937.
(32) Mairesse, G.; Roussel, P.; Vannier, R.-N.; Anne, M.; Pirovano, C.; Nowogrocki, G. *Solid State Sci.* **2003**, *5*, 851–859.

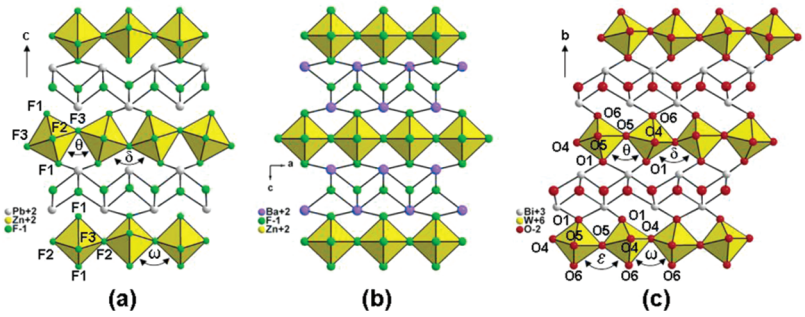

Figure 11. Section of the crystal structures of (a) β-Pb_2ZnF_6, (b) Ba_2ZnF_6, and (c) LT-Bi_2WO_6 along the (1−10), (010), and (101) planes, respectively.

This layered two-dimensional type structure is built up from fluorite-like slabs ($(Pb_2F_2)^{2+}$ in β-Pb_2ZnF_6 and $(Bi_2O_2)^{2+}$ in LT-Bi_2WO_6) parallel to the (*a*,*b*) plane alternating along the *c*-axis with single perovskite-like block ($[ZnF_4]^{2-}$ in β-Pb_2ZnF_6 and $[WO_4]^{2-}$ in LT-Bi_2WO_6) of corner-sharing octahedra. It must be noted that these perovskite slabs are strongly corrugated in both phases when compared with the prototype I 4/mmm structure (Ba_2ZnF_6[33] in Figure 11). In β-Pb_2ZnF_6, (space group P 4_2/ncm), the magnitude of the antiphase tilting angle $\phi = 17.268°$ within these $[ZnF_4]^{2-}$ slabs is calculated using the following formula: $\phi = \arctan\left[z_{F3}.c/\sqrt{2(1/4.a)^2}\right]$, with z_{F3} the *z*-coordinate of F3 atoms, *a* and *c* the unit cell parameters.

The octahedron antiphase tilting in consecutive $[ZnF_4]^{2-}$ perovskite layers of β-Pb_2ZnF_6, are in opposite sense and alternatively along the *a*-axis and the *b*-axis of the prototype structure of Ba_2ZnF_6 ($\phi = 0$), both having the equally large magnitude ϕ. Thereby, the tilting scheme in β-Pb_2ZnF_6 is (ϕ00)(0-ϕ0) according to the standard notation proposed by Aleksandrov et al.[34] In order to give an insight into the origin of this tilting, let us examine first the fluorine environment of Pb^{2+} ion in β-Pb_2ZnF_6. In the structure of Ba_2ZnF_6, barium atom resides at the center of a regular BaF_8^{6-} square antiprism formed by apical fluorine corners of four untilted ZnF_6^{4-} octahedra and four fluorine atoms located in $(Ba_2F_2)^{2+}$ slab. Although the Pb^{2+} ion has a smaller size than the Ba^{2+} ion,[35] no reduction of the inter-perovskite blocks distance (determined from apical anion sites in two consecutive blocks) is observed in β-Pb_2ZnF_6 (4.195 Å) when compared to that of Ba_2ZnF_6 (4.196 Å). This is ascribed to the spatial extension of the $6s^2$ lone pair (E) of divalent lead cation directing toward single $[ZnF_4]^{2-}$ perovskite−like blocks. In β-Pb_2ZnF_6, the steric effect of the lone pair moves apart apical F1 corners of two over four neighboring ZnF_6^{4-} octahedra, leading to the formation of only two strong Pb−F1 bonds (d = 2.535 Å, materialized in Figure 11a) and thereby to a highly asymmetric fluoride coordination environment for Pb^{2+} ion, noted $[PbF_6E]$ considering the shortest Pb−F distances ($d_{Pb-F} < 2.56$ Å). The consequences are the following: (i) The patent deformation of the Ba_2ZnF_6 prototype structure (Figure 11b) by a strong octahedron tilting in $[ZnF_4]^{2-}$ perovskite blocks. In β-Pb_2ZnF_6,inter-octahedral F1−F3−F1 bond angles are alternatively smaller and larger than 90° ($\theta = 61.6°$ and $\delta = 122.3°$ in Figure 11a), while inter-octahedral F1−F2−F1 bond angles remain close to 90° ($\omega = 92.2°$ in Figure 11a). This tilting reduces significantly the *a* tetragonal cell (Z = 4, a = 5.633 Å)[10] parameter in β-Pb_2ZnF_6 when compared to the length of the diagonal in the (*a*,*b*) plane of Ba_2ZnF_6 (Z = 2, $\sqrt{2}a$ = 5.780 Å, taking into account the change in cell orientation).[33] (ii) the intra-distortion of ZnF_6^{4-} octahedron. The equatorial F2 and F3 corners, shared between two octahedra in the (*a*,*b*) plane, are also the fluorine ions having the shortest (1.991 Å) and longest (2.085 Å) Zn−F distances, respectively. However, the zinc atom is not off-centered although F1−Zn−F3 bond angles are different from 90°.

The deformation of single perovskite blocks in the LT-form of Bi_2WO_6 (Figure 11c) is also involved by the lone pair Bi^{3+} cation. However, the situation is more complex since rotation of the WO_6^{6-} octahedra takes place around both the *b* and *c* axes within a single perovskite block together with lateral displacements of these octahedra. This is clearly highlighted by the deviation from 90° of both inter-octahedral O1−O4, 5−O1 and O6−O4, 5−O6 bond angles ($\theta = 80.1°$, $\delta = 107.3°$, $\varepsilon = 107.6°$ and $\omega = 77.3°$ in Figure 11c). It is worth mentioning that WO_6^{6-} octahedron is also distorted in LT-Bi_2WO_6 with the shortest and longest W−O distances involving equatorial O4 and O5 atoms, as observed in β-Pb_2ZnF_6. However, the magnitude of the octahedral distortion is larger in LT-Bi_2WO_6 than that observed in the fluoride due to the off-centering of W^{6+}. An atomistic simulation was performed on LT-Bi_2WO_6 in order to get better insight into the oxide ion migration mechanism.[29] This study revealed that the lowest energy pathway for migration involves apical O1,6 and equatorial O4,5 sites of the WO_6^{6-} octahedra. This preferential zig-zag type pathway then takes place within the single $[WO_4]^{2-}$ perovskite-like block. Exchange between these oxygen sites was later confirmed by ^{17}O MAS NMR spectroscopy.[36] Above 200 °C, the 1D variable temperature ^{17}O MAS NMR spectra of $Bi_2W_{0.9}Nb_{0.1}O_{5.95}$ show a coalescence of the resonances assigned to apical O1,6 and equatorial O4,5

(33) Von Schnering, H. G. *Z. Anorg. Allg. Chem.* **1967**, *353*, 13–25.
(34) Aleksandrov, K. S.; Bartholomé, J. *J. Phys.: Condens. Matter* **1994**, *6*, 8219–8235.
(35) Shannon, R. D. *Acta Crystallogr. A* **1976**, *32*, 751–767.
(36) Kim, N.; Vannier, R.-N.; Grey, C. P. *Chem. Mater.* **2005**, *17*, 1952–1958.

oxygen of the WO_6^{6-} octahedron due to the exchange between these oxygen sites (correlation time $\tau_c = 3.3 \times 10^{-5}$ s at 225 °C). Concomitantly, conductivity can be measured by complex impedance spectroscopy above this temperature. As the temperature still increases, cross peaks starts to emerge in 2D ^{17}O MAS NMR spectra between the resonances of oxygen atoms in perovskite-like $[WO_4]^{2-}$ blocks and in fluorite-like $(Bi_2O_2)^{2+}$ slabs. This latter site exchange (correlation time $\tau_c = 12-22 \times 10^{-3}$ s at 225 °C) has a weak contribution to oxygen transport since the exchange within single perovskite blocks is several hundred times faster.

The patent similarity with the current ^{19}F MAS NMR study performed on β-Pb_2ZnF_6 originates from the structural correlation. However, in β-Pb_2ZnF_6, both anion site (intra-perovskite blocks F1−F2,3 and F1−F5 between perovskite blocks/fluorite slabs) exchanges occur at lower temperatures and with shorter correlation times than observed in Bi_2WO_6 based oxide ion conductors although that F1−F5 distances in β-Pb_2ZnF_6 ($d_{F1-F5} = 2.72$ Å) are similar to O6−O3 and O1−O2 distances in Bi_2WO_6 (2.75 Å for both). This is mainly due to the smaller size of the F^- ion compared to that of O^{2-} ion and to the higher polarizability of Pb^{2+} ion compared to that of Bi^{3+} ion (6.58 $Å^3$ and 6.12 $Å^3$,[37] respectively). From a purely geometrical point of view, the higher exchange between perovskite blocks/fluorite slabs in β-Pb_2ZnF_6 could be ascribed to the reduction of the inter-perovskite blocks from 4.606 Å in Bi_2WO_6 to 4.195 Å in β-Pb_2ZnF_6 (distance determined from *y* and *z* coordinates of apical anion sites in two consecutive blocks, respectively). In the light of the above structural considerations and of the NMR experiments, the anionic conduction measured in the temperature range 170−280 °C by complex impedance spectroscopy in β-Pb_2ZnF_6 is clearly tridimensional in nature.

(37) Shannon, R. D. *J. Appl. Phys.* **1993**, *73*, 348–366.

4. Conclusion

In this work, we have reported an investigation of the fluoride ion mobility in $Pb_5Ga_3F_{19}$ and β-Pb_2ZnF_6 using VT 1D solid-state ^{19}F MAS NMR and 2D exchange NMR experiments, temperature-controlled X-ray diffraction, and impedance spectroscopy measurements. The results revealed specific details on the anion site exchange dynamics and the combined use of these techniques offered the potentiality to discuss the behavior of each fluoride ion individually. In both compounds, the motion of fluoride ions involves anion vacancies. In $Pb_5Ga_3F_{19}$, a chemical exchange between all fluoride sites within the isolated $Ga1F_6^{3-}$ octahedra and between these ions and some of the free fluoride ions is observed. The exchange does not involve all the fluoride ions. Due to this non-diffusive process, no anionic conductivity was detected. In the Aurivillius phase type compound β-Pb_2ZnF_6, we show that the thermal behavior depends on the sample. In one of the two studied β-Pb_2ZnF_6 samples, NMR results show two distinct chemical exchanges: a first one, bidimensional, that occurs in the ZnF_6^{4-} octahedron layers, and a second one, tridimensional, that involves a part of the fluoride ions of all the crystallographic sites. By extrapolation of the ^{19}F NMR data, the totality of the fluoride ions is estimated to be mobile above 160 °C. If the sample partly decomposes for temperature higher than 280 °C, impedance spectroscopy measurements nevertheless reveal, as expected from ^{19}F NMR, interesting anionic conductivity properties in β-Pb_2ZnF_6 for temperature in the range 170−280 °C.

Acknowledgment. We thank an anonymous referee for constructive remarks on the manuscript.